Submitted to the
17th International Conference on Ground Penetrating Radar,
June 18–21, 2018 in Rapperswil, Switzerland

Quantifying scour depth in a straightened gravel-bed river with ground-penetrating radar

Emanuel Huber
Birte Anders
Peter Huggenberger
Applied and Environmental Geology
University of Basel
4056 Basel, Switzerland
emanuel.huber@unibas.ch, birte.anders@unibas.ch, peter.huggenberger@unibas.ch

***Abstract*—In straight gravel-bed river reaches, riverbank erosion can be induced by alternate bars and their associated scours. The maximum scour depth is therefore a key information to design reliable flood protections. However, scour depth cannot be correctly assessed by bathymetric riverbed surveys if scours are filled with sediments at low discharge. In this work, scour depths in a straightened, gravel-bed river with alternate bars is quantified with ground-penetrating radar (GPR) and the riverbed morphology is linked to the subsurface structure. A 4.5 m deep buried scour with an extent of 30 × 100 m is partially imaged by GPR at the front end of the gravel bar next to the riverbank. The non-imaged part of the scour is expected to be much larger and therefore deeper. Additional research is needed to assess how scour location and depth relate with discharge magnitude and gravel bar dynamics.**

Keywords—ground-penetrating radar; gravel-bed river; scour; alternate bar; sedimentoloty; flood protection

I. Introduction

In the last centuries, many rivers worldwide were channelized and straightened to prevent lateral erosion of the riverbank as well as flooding. The engineers believed that straightening river stretches would maintain flat riverbeds reducing riverbank erosion [1]. However, alternate bars appeared in many rivers with reduced riverbed width [2] and specific grain-size – river-width relation [3]. Alternate bars are elongated bedforms that emerge at low discharge and alternatively occur at the left and right riverbank (Fig. 1).

Through laboratory experiments on alternate bars, [4,5] could demonstrate that each alternate bar is associated with a local scour (also called pool) immediately upstream (Fig. 1, see also [6-8]). At high river discharge, alternate bars and their associated scours are expected to migrate downstream over several hundreds of meters [9]. Because the scour depths range up to four times the water depth at medium discharge [10], the stability of riverbank is therefore threatened by the migration of such deep scours close to the riverbank [3]. Furthermore, several studies showed that alternate bars in straightened channels induce lateral erosion and could initiate channel meandering or braiding [5,11-14].

In Switzerland, the risk for riverbank erosion was underestimated until August 2005, when many riverbanks and levees collapsed during a supra-regional flood [15]. This 100-year flood cost the life of six people and caused damage of approximately three billion Swiss francs. Such flood events are not unique in history and similar or even larger flood events are

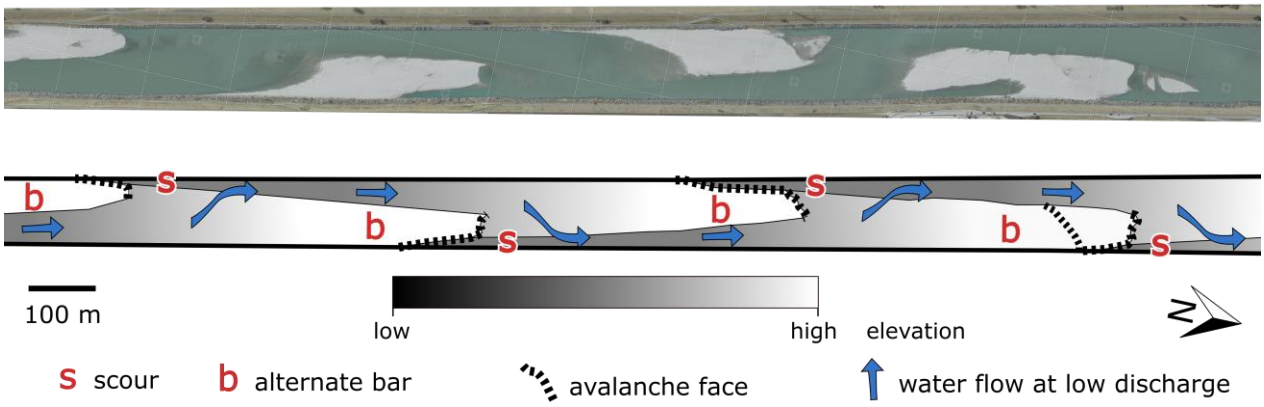

Fig. 1. Top: aerial photograph of the Alpine Rhine River with alternate bar (100 m downstream from the study site). Bottom: morphological interpretation of the aerial photograph with low-discharge water flow path.

TABLE I. GPR PROCESSING STEPS

Processing step	Description/literature
DC-shift removal	Remove constant amplitude shift.
First-breaks picking and time-zero adjustment	E.g., [16].
Constant offset correction	Compensate for the 1-m-offset between transmitter and receiver antennae (the acquisition time of the traces is converted into the corresponding acquisition time for a mono-static antenna GPR).
Low-frequency trend removal (dewow)	Low-frequency trend estimated with a Hampel filter (e.g., [17]).
Band-pass frequency filtering	Remove the low and high noisy frequencies (corner frequencies: 5, 25, 150, 250 MHz).
Spherical and exponential amplitude corrections	Compensate for geometric spreading and attenuation of the GPR signal (e.g., [18-19]).
2D median filtering	Applied over a 3-by-3 neighborhood to remove high-frequency noise.
Topographic Kirchhoff migration	Topographic Kirchhoff migration [20-21] with constant GPR wave velocity (0.1 m/ns) that leads to results that are accurate enough for the purpose of the study.
Automatic Gain Control	Adaptative amplitude correction (e.g., [22]).

expected in the future. Therefore, understanding the mechanism of scour formation in the context of gravel bar migration during large floods is crucial to designing reliable riverbank protection measures as well as to developing comprehensive flood protection policies.

Maximal scour depth is a critical parameter to design reliable flood embankment. But the maximal scour depths estimated at low to medium discharges from riverbed surveys are not necessarily representative of the real maximal erosion depths. At high discharge, scours are partly buried by the preceding alternate bars while both scours and bars migrate downstream. During the flow recession, scours are partly or fully filled with sediments and their erosion base lie clearly below the riverbed at low discharge [23].

The erosional surfaces of buried scours can be portrayed by ground-penetrating radar (GPR), a high-resolution, non-destructive geophysical device to image subsurface. Many studies focused on the use of GPR to assess bridge scour holes [24] or to characterize the subsurface structure of gravel deposits (e.g., [25-26]). The near-surface morphological and depositional elements were intensively described in the literature ([9] and references therein). However, there is little knowledge on the formation and migration of scours at high discharge and on their footprints left in the subsurface deposits.

This contribution aims to quantify scour depths in a straightened, gravel-bed river with alternate bars and relate riverbed morphology to subsurface structure based on GPR measurements.

Because this study focuses on the dynamic interaction of scour and bedform development, the sedimentological term ‘gravel sheet’ ([25,27]) is preferred over the morphological term ‘bar’ (see [28], p.149). The former is more adequate to relate GPR reflection patterns to the interplay scour-gravel sheet development.

A series of GPR data were collected on a 200 × 60 m gravel sheet of the Alpine Rhine River up to Lake Constance (Switzerland). Lower bounding surfaces of scours were first identified and delineated on the GPR data. Finally, the interpretation lines were interpolated into surfaces from which the erosion depths are quantified. Furthermore, the propagation direction of gravel sheets and scours formation were inferred from the orientation of the reflections within the erosion surfaces.

II. METHODS

A. GPR data acquisition

GPR data were acquired with a PulseEkko Pro GPR device (manufactured by Sensors and Software, Inc., Mississagua, Ontario) with a pair of unshielded 100-MHz antennae separated by 1 m. The recording of the GPR waves at regular intervals along the survey lines was triggered by an odometer every 0.2 m. The GPR survey was conducted on top of a 200 × 60 m emerged gravel sheet. There, the riverbed (i.e., the channel) is about 100 m wide (Fig. 2). Furthermore, a smaller

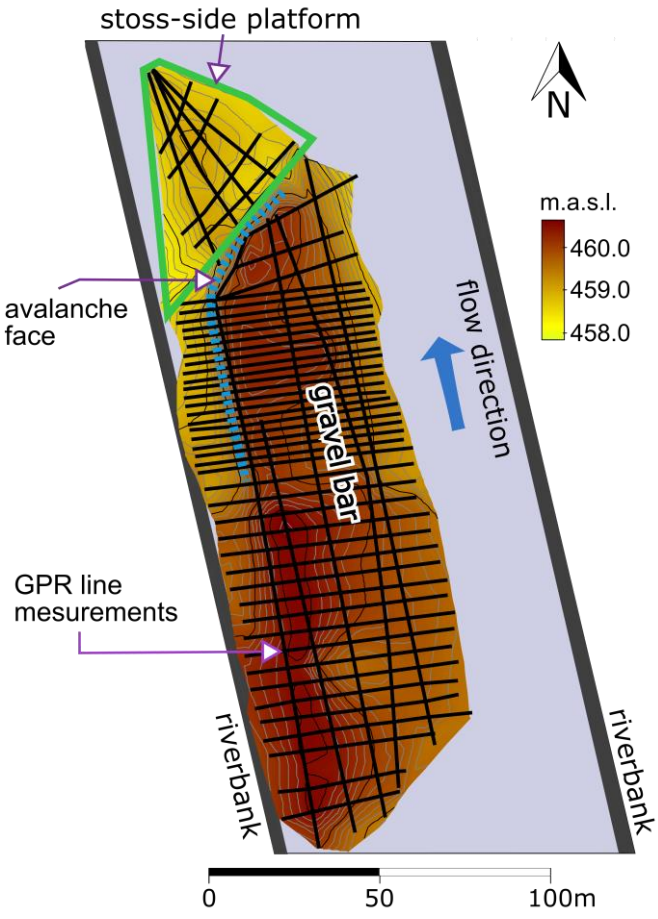

Fig. 2. GPR survey (black lines) superimposed on the surveyed topography of the gravel bar.

grid of 4 × 4 GPR lines (40 × 50 m) was recorded downstream the gravel bar. Two common mid-point (CMP) data were recorded to estimate the mean electromagnetic wave velocity [29-31]. The position of the GPR lines, the topography of the survey area and the edge of the water surfaces were surveyed with a total station (South, NTS 355L). The GPR profiles parallel (perpendicular, respectively) to the general flow direction within the survey area are called along-flow (across-flow, respectively) profiles.

B. GPR data processing

GPR data processing aims to increase the signal-to-noise ratio without introducing artefacts in the data. The data are processed with the R-package RGPR [32] (see processing workflow in TABLE I). The processed GPR data are then imported in GOCAD (Paradigm) for interpretation and surface interpolation.

C. GPR data interpretation

The interpretation of the GPR profiles is based on (i) continuity of the dominant reflections within and between the profiles, (ii) differences of reflection patterns, and (iii) angular unconformity between the reflections that can indicate an erosion surface or the superposition of two sedimentary structures with different sedimentary textures [33-34].

Erosional lower bounding surfaces (i.e., scour surface) are first identified and delineated on the along-flow profiles. Then, the across-flow profiles are used to control and correct the interpretation. Finally, the interpretation lines are interpolated into surfaces corresponding to lower-bounding erosion surfaces. Only non-ambiguous structures are interpreted. For each surface, the maximum erosion depth is estimated. Because some of the erosion surfaces are not entirely preserved, the real maximum erosion depth can be larger than the estimates. Furthermore, the direction of sediment deposition is inferred from the orientation of the reflections within the erosion surfaces.

III. Results and Discussion

A. Alternate gravel sheets

The gravel sheet is up to 2 m thick with a sharp avalanche face at its downstream end toward the riverbank (Fig. 2). The orientation of the avalanche face indicates the direction of the most recent gravel sheet migration. The area downstream the gravel sheet, called stoss-side platform by [35], is rather flat and its surface consists in fine sediments, mainly sand.

The base of the gravel sheet is well identified on the GPR data by a strong and continuous reflection that is discordant with the reflections below. This reflection presumably corresponds to the armor layer found below gravel sheet (e.g., [36]). Within the gravel sheet deposits, two concordant layers are resolved by GPR suggesting that the gravel sheet consists in fact of (at least) two superimposed gravel sheets. In the top layer, some foresets directed at -45° to the main flow direction are observed at some locations indicating the gravel sheet propagation direction toward the riverbank (Fig. 3). This propagation direction corresponds to the orientation of the avalanche face and suggests that the top gravel sheet climb onto a preexisting gravel sheet. The decreasing thickness of the top layer toward the left riverbank (i.e., decreasing foresets length) can result from the erosion of its upper part.

The top part of the gravel sheet may have been eroded as indicated in Fig. 3 by the decreasing size of the foreset toward the left riverbank.

B. Deep scour close to the riverbank

A deep erosion surface (Fig. 4) is identified between the riverbank and gravel sheet where scours are expected to be found (compare Fig. 1 with Fig. 4, see also [37]. The interpreted erosion surface is up to 30 m wide, more than

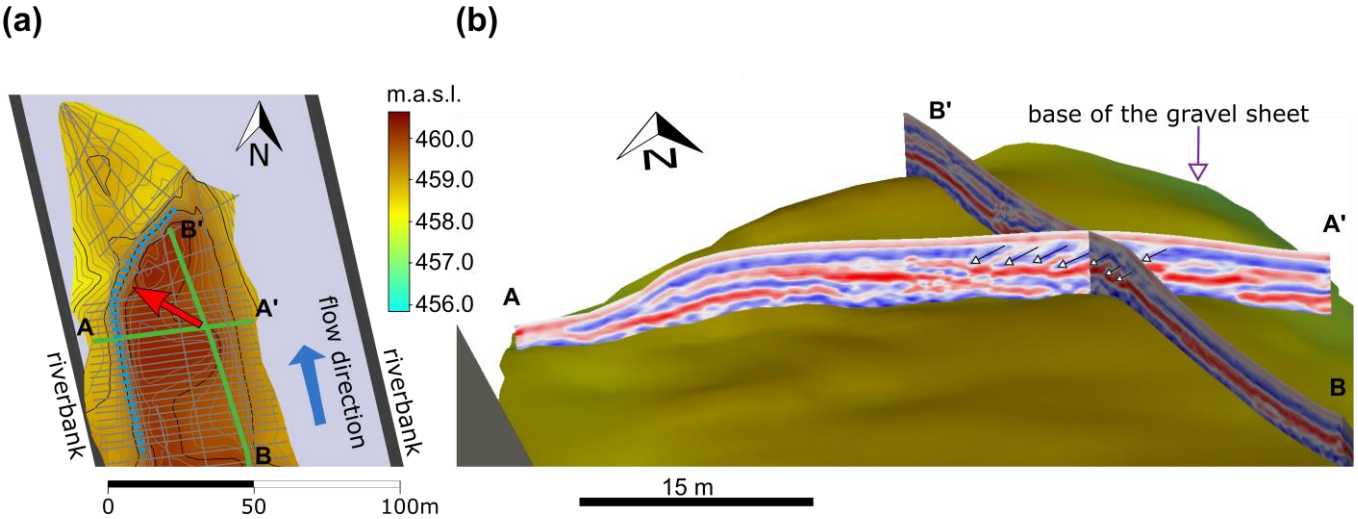

Fig. 3. a) Top view of the gravel bar with two perpendicular GPR profiles (green lines), the small red arrow indicates the direction of the foresets of the gravel sheet observed in b). b) Surface and base of the gravel sheet. On the two perpendicular GPR profiles, foresets are clearly visible within the gravel sheet (indicated by a series of black arrows).

100 m long and 4.5 m deep (elevation difference) but the real erosion surface is expected to be much larger and deeper, especially close to the riverbank. The elevation difference between the highest point of the gravel sheet surface and the deepest point of the erosional surface is 7.4 m. In comparison, [9] estimated the riverbed elevation difference of the Alpine Rhine River to range between 2.5 m and 4 m. This estimation based on cross-section surveys (average spacing 200 m) clearly underestimates the real scour depths.

Note that the erosion surface already starts to deep below the gravel sheet 10 to 15 m upstream the gravel sheet avalanche face (Fig. 4.a). This spatial shift between the erosional surface and the avalanche face could result from a joint migration of the gravel sheet and scour. Furthermore, the GPR reflections within the erosion surface show an onion-like pattern: a series of curved, concave reflections are observed. Such pattern can arise from a net sediment deposition in the scour (aggradation). It remains however unclear if the scour was filled before the avalanche face was formed.

This finding corroborates previous research on alternate gravel sheets and associated scours [3-4,6-8] and highlights the presence of deep, buried scours close to the riverbank. The deep scour in Fig. 4 has been only partially imaged by GPR and therefore its size is expected to be much larger. Furthermore, the scour sizes are presumably related to the discharge magnitude: extreme high discharge event can scour the riverbed much deeper.

C. A highly dynamic environment

Other smaller erosional lower bounding surfaces (up to 3 m deep) were identified at lower depths. Their origins remain unclear but they can be remnants of scours, either from the channelized Rhine River or from the depositional environment prior to the channelization. Therefore, their original depths are rather uncertain.

The absence of foresets below the gravel sheet base indicates a low preservation potential of the gravel sheets: they are not preserved in the deposits as intact gravel sheets but only as remnants (i.e., as reworked gravel sheets). The presence of scour remnants combined with the absence of gravel sheet foresets as well as a large number of short discontinuous reflections are the mark of a highly dynamic depositional environment characterized by a high rate of erosional processes. It is therefore very challenging to provide an interpretation of the subsurface structures at lower depths without having a direct link to the former morphology or depositional system.

IV. Conclusion

This work demonstrates how GPR studies can contribute to better flood protection measures in a straightened river with alternate gravel sheet through a deeper appreciation of the sedimentological processes. The GPR data showed the presence of a more than 4.5 m deep scour close to the riverbank, downstream the gravel sheet. Bathymetric survey measurements cannot assess the depth of such filled scours and therefore they tend to underestimate the maximal scour depth, a critical parameter for flood embankment design. Repeated GPR measurements on exposed gravel sheets could provide better insight into how scour location and depth relate with discharge magnitude and gravel sheet dynamics.

During gravel sheet and scour migration, the hydrodynamic processes produce distinct sediment sorting that results in contrasting sedimentary textures (e.g., poorly sorted gravel of the gravel sheets vs. highly permeable gravel layers within the scour fills [28]). These sedimentary textures do not only impact bedform stability but also benthic macroinvertebrate abundance as well as river water – groundwater interaction. GPR studies could contribute to a better understanding of these processes that have been not yet fully explored.

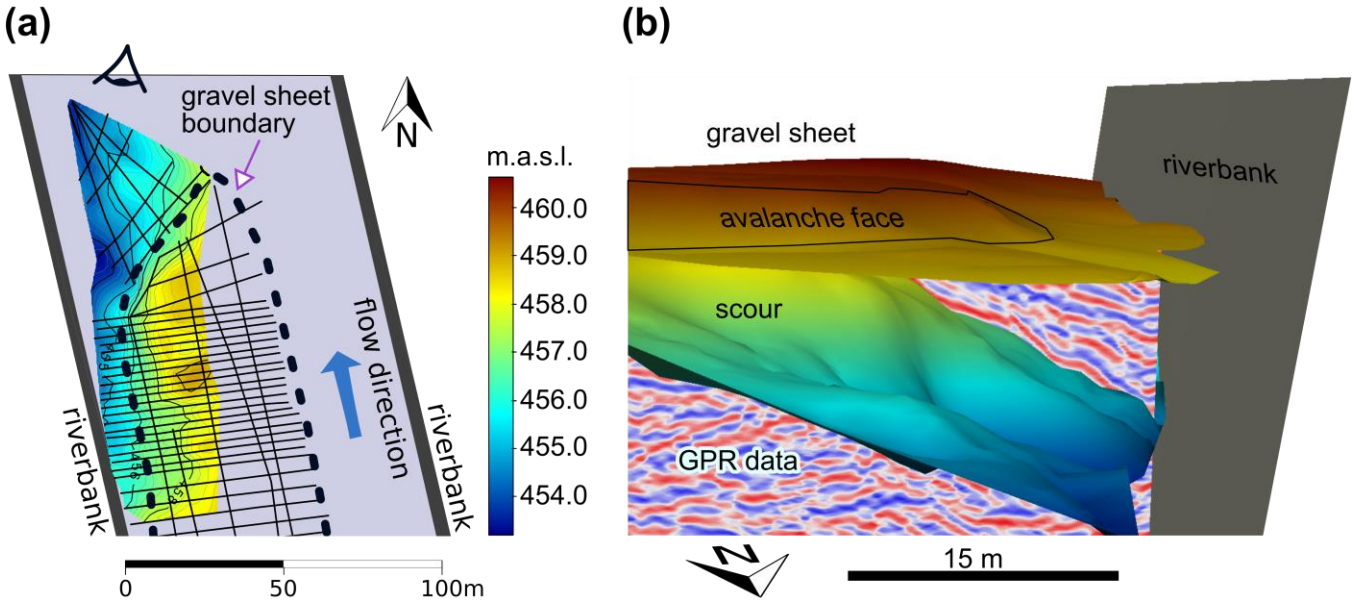

Fig. 4. a) Elevation map of the erosional lower bounding surface of a scour. b) Gravel sheet surface elevation and erosional lower bounding surface of the scour shown in a) with GPR data.

ACKNOWLEDGMENT

Work by the first author was partially funded by the Swiss National Science Foundation (grants no. CRSI22_132249/1 and P2BSP2_161955).

REFERENCES

[1] A. von Salis, Das Schweizer Wasserbauwesen, Staempflische Buchdruckerei, Bern, 1833.

[2] H. Grebenau, Der Rhein vor und nach seiner Regulierung auf der Strecke von der Lauter bis Germersheim, XXVIII. Und XXIX. Jahresbericht der Pollichia, eines naturwissenschaftlichen Vereines der Rheinpfalz, Dürkheim a.d.H., 1870.

[3] M. Jäggi, Formation and effects of alternate bars, J. Hydraul. Eng., 110(2), pp. 142-156, February 1984. doi:10.1061/(ASCE)0733-9429(1984)110:2(142).

[4] P. E. Ashmore, Laboratory modelling of gravel braided stream morphology. Earth Surf. Process. Landforms, 7, pp. 201-225, May 1982. doi:10.1002/esp.3290070301

[5] P. E. Ashmore, Process and Form in Gravel Braided Streams: Laboratory Modelling and Field Observations, Ph.D. Thesis, University of Alberta, 414 pp., 1985.

[6] S. Ikeda, Prediction of Alternate Bar Wavelength and Height. Journal of Hydraulic Engineering 110(4), pp. 371-386, April 1984. doi:10.1061/(ASCE)0733-9429(1984)110:4(371)

[7] R. S. Pyrce, and P. E. Ashmore, Particle path length distribution in meandering gravel-bed streams: Results from physical models. Earth Surface Processes and Landforms, 28, pp. 951-966, July 2003. doi:10.1002/esp.498

[8] A. R. Bankert, and P. A. Nelson, Alternate bar dynamics in response to increases and decreases of sediment supply. Sedimentology, August 2017, in press. doi:10.1111/sed.12399

[9] L. Adami, W. Bertoldi, and G. Zolezzi, Multidecadal dynamics of alternate bars in the Alpine Rhine River, Water Resources Research, 52, pp. 8938-8955, November 2016. doi:10.1002/2015WR018228.

[10] M. Jaeggi, Alternierende Kiesbänke (Alternate bars), PhD thesis, Swiss Federal Institute of Technology Zurich, Diss. ETH Nr. 7208, Switzerland, 286 pp., 1983.

[11] F. M. Exner, Über die Wechselwirkung zwischen Wasser und Geschiebe in Flüssen, Sitzungsberichte der Akademie der Wissenschaften mathematisch-naturwissenschaftliche Klasse 134_2a, Wien, pp. 165-203, 1925.

[12] D. B. Simons, and E. V. Richardson, Flow in alluvial sand channels. In River Mechanics, H. W. Shen, Ed., Fort Collins, Colorado, Chapter 9, 1971.

[13] J. Lewin, Initiation of bedforms and meanders in coarse grained sediment, Bull. Geol. Soc. Am., 87(2), pp. 281-285, February 1976. doi: 10.1130/0016-7606(1976)87<281:IOBFAM>2.0.CO;2

[14] G. Parker, On the cause and characteristic scales of meandering and braiding in rivers, J. Fluid Mech., 76(3), pp. 457-480, August 1976. doi:10.1017/S0022112076000748.

[15] L. Hunzinger, A. Bachmann, R. Brändle, P. Dändliker, D. Jud, and M. Koksch, Empfehlung zur Beurteilung der Gefahr von Ufererosion an Fliessgewässern. Kommission für Hochwasserschutz KOHS des Schweizerischen Wasserwirtschaftsverband SWV, Fachleute Naturgefahren Schweiz FAN, October 2015.

[16] J. I. Sabbione, and D. Velis, Automatic first-breaks picking: New strategies and algorithms, Geophysics, 75(4), pp. 67-76, July 2010. doi:10.1190/1.3463703

[17] R. K. Pearson, Outliers in process modeling and identification, IEEE Transactions on Control Systems Technology, 10(1), pp. 55-63, January 2002. doi:10.1109/87.974338

[18] S. Kruse, and H. M. Jol, Amplitude Analysis of Repetitive GPR Reflections on A Lake Bonneville Delta, Utah. In: Bristow, C.S. and Jol, H. M. (eds), GPR in Sediments, Geological Society of London, Special Publication 211, pp. 287–298, 2003. doi: 10.1144/GSL.SP.2001.211.01.23

[19] R. E. Grimm, E. Heggy, S. Clifford, C. Dinwiddie, R. McGinnis, and D. Farrell, Absorption and scattering in ground-penetrating radar: Analysis of the Bishop Tuff, J. Geophys. Res., 111, E06S02, March 2006. doi:10.1029/2005JE002619

[20] F. Lehmann and A. G. Green, Topographic migration of georadar data. Proc. SPIE 4084, Eighth International Conference on Ground Penetrating Radar, 5 pp., April 2000. doi:10.1117/12.383556

[21] J.-R. Dujardin and M. Bano, Topographic migration of GPR data: Examples from Chad and Mongolia. Comptes Rendus Geoscience, 345(2), pp. 73-80, February 2013. doi:10.1016/j.crte.2013.01.003

[22] O. Yilmaz, Seismic Data Analysis: Processing, Inversion, and Interpretation of Seismic Data. Investigation in Geophysics no. 10, Society of Exploration Geophysics, 2001. doi: 10.1190/1.9781560801580

[23] Y. Storz-Peretz, and J. B. Laronne, Morphotextural characterization of dryland braided channels. GSA Bulletin, 125(9/10), p. 1599–1617, September/October 2013. doi: 10.1130/B30773.1 2013

[24] G. Placzek, and F. P. Haeni, Surface-geophysical techniques used to detect existing and infilled scour holes near bridge piers. Federal Highway Administration, Dept. of the Interior, U.S. Geological Survey, 44 pp., 1995.

[25] P. Huggenberger, E. Hoehn, R. Beschta, W. Woessner, Abiotic aspects of channels and floodplains in riparian ecology. Freshwater Biology, 40(3), pp. 407-425, November 1998.

[26] H. Okazaki, Y. Kwak, and T. Tamura, Depositional and erosional architectures of gravelly braid bar formed by a flood in the Abe River, central Japan, inferred from a three-dimensional ground-penetrating radar analysis, Sedimentary Geology, 324, pp. 32-46, July 2015. doi: 10.1016/j.sedgeo.2015.04.008

[27] E. Huber, and P. Huggenberger, Morphological perspective on the sedimentary characteristics of a coarse, braided reach: Tagliamento River (NE Italy). Geomorphology, 248, pp. 111-124, November 2015. doi: 10.1016/j.geomorph.2015.07.015

[28] C. Siegenthaler, and P. Huggenberger, Pleistocene Rhine gravel: deposits of a braided river system with dominant pool preservation. In J. L. Best, and C. S. Bristow (eds.) Braided Rievers, Geological Society, London, Special Publications, 75, pp. 147-162, January 1993. doi: 10.1144/GSL.SP.1993.075.01.09

[29] C. H. Dix, seismic velocities from surface measurements. Geophysics, 20(1), pp. 68-86, January 1955. doi:10.1190/1.1438126 1955;

[30] S. Tillard, and J.-C. Dubois, Analysis of GPR data: wave propagation velocity determination. Journal of Applied Geophysics, 33(1-3), pp. 77-91, January 1995. doi: 10.1016/0926-9851(95)90031-4

[31] A.D. Booth, R. Clark, and T. Murray, Semblance response to a ground-penetrating radar wavelet and resulting errors in velocity analysis. Near Surface Geophysics, 8(3), pp. 235-246, June 2010. doi:10.3997/1873-0604.2010008

[32] E. Huber, and G. Hans, "R-package with S4 classes for ground-penetrating radar (GPR) data visualization, analysis, and processing", https://github.com/emanuelhuber/RGPR, consulted on January 17th, 2018.

[33] M. Beres, A. G. Green, P. Huggenberger and H. Horstmeyer, Mapping the architecture of glaciofluvial sediments with three-dimensional georadar. Geology, 23(12), pp. 1087-1090, December 1995. doi: 10.1130/0091-7613(1995)023<1087:MTAOGS>2.3.CO;2

[34] M. Beres, P. Huggenberger, A. G. Green and H. Horstmeyer, Using two- and three-dimensional georadar methods to characterize glaciofluvial architecture. Sedimentary Geology, 129(1–2), pp. 1-24, November 1999. doi: 10.1016/S0037-0738(99)00053-6

[35] S. P. Rice, M. Church, C. L. Wooldridge and E. J. Hickin, Morphology and evolution of bars in a wandering gravel-bed river; lower Fraser river, British Columbia, Canada. Sedimentology, 56(3), pp. 709-736, April 2009. doi: 10.1111/j.1365-3091.2008.00994.x

[36] R. Müller, Theoretische Grundlagen der Fluss- und Wildbachverbauungen. Mitteilung der Versuchsanstalt für Wasser- und Erdbau, ETH Zürich, 4, 1943.

[37] R. S. Eilertsen, and L. Hanson, Morphology of river bed scours on a delta plain revealed by interferometric sonar. Geomorphology, 94(1), pp. 58-68, February 2008. doi:10.1016/j.geomorph.2007.04.00